HORIZON EUROPE PROGRAMME
HORIZON-CL4-2023-DIGITAL-EMERGING-01-33

GA No. 101135196

Developing New 2D Materials and Heterostructures for Printed Digital Devices

2D-PRINTABLE - Deliverable report

D4.1– Characterization of nanosheets, networks and heterostacks built from initially available 2D materials

Funded by
the European Union

Deliverable No.	D4.1	
Related WP	WP 4	
Deliverable Title	Characterization of nanosheets, networks and heterostacks built from initially available 2D materials	
Deliverable Date	30.09.2024	
Deliverable Type	REPORT	
Dissemination level	Public (PU)	
Author(s)	Claudia Backes (UKa) Jonathan N Coleman (TCD)	2024-09-14
Checked by	Claudia Backes (UKa)	2024-09-14
Reviewed by	Georg Duesberg (UniBWM) Zdenek Sofer (VSCHT)	2024-09-17
Approved by	Jonathan Coleman (TCD) - Project Coordinator	30.09.2024
Status	Final	30.09.2024

Document History

Version	Date	Editing done by	Remarks
V1.0	06.09.2024	Jonathan Coleman	
V1.1	14.09.2024	Claudia Backes	
V2.0	17.09.2024	Georg Duesberg	
V3.0	20.09.2024	Zdenek Sofer	
FINAL			

Project Scientific Abstract

The 2D-PRINTABLE project aims to integrate sustainable large-scale liquid exfoliation techniques with theoretical modelling to efficiently produce a wide range of new 2D materials (2DMs), including conducting, semiconducting, and insulating nanosheets. The focus includes developing the printing and liquid phase deposition methods required to fabricate networks and multicomponent heterostructures, featuring layer-by-layer assembly of nanometer-thick 2DMs into ordered multilayers. The goal is to optimize these printed networks and heterostructures for digital systems, unlocking new properties and functionalities. The project also seeks to demonstrate various printed digital devices, including proof-of-principle, first-time demonstration of all-printed, all-nanosheet, heterostack light-emitting diodes (LEDs). In conclusion, 2D-PRINTABLE will prove 2D materials to be an indispensable material class in the field of printed electronics, capable of producing far-beyond-state-of-the-art devices that can act as a platform for the next generation of printed digital applications.

Public summary

The report outlines the progress made regarding the characterisation of initially available 2D materials, as well as their printed networks and heterostacks. While an abundance of layered materials have been theoretically predicted to exist, only a fraction of them has been successfully exfoliated and characterised. Upon exfoliation, it is crucial to assess if the predicted physicochemical properties of the produced nanosheets have been preserved and are retained in solution for further processing. Furthermore, the development of characterisation techniques to quantify the morphological properties of solution-processed networks made from 2D materials will be crucial for device applications. This is an area of intensive research and forms the basis of the work described in this report.

We first will present the characterisation results on liquid phase exfoliated (LPE) and electrochemically exfoliated (EE) nanosheets, such as MoS_2, $AsSbS_3$, As_2S_3, SnGe, InSe, $Mo_{0.5}W_{0.5}Se_2$, and $HfSe_3$. Using atomic force microscopy (AFM), it was determined that the aspect ratio (AR) of EE nanosheets can reach values > 10^3, which is nearly 30 times larger than those obtained by the LPE method (AR ~ 10 - 30). Further characterisation by UV-Vis and Raman spectroscopy was used to investigate the intrinsic properties of the produced nanosheets. For EE MoS_2, we began to explore whether information on dimensions or doping is potentially accessible from extinction spectroscopy.

The Langmuir-Schaefer (LS) method is believed to be an ideal method to fabricate ultra-thin and uniform nanosheet networks. However, the morphology of such networks is difficult to measure quantitatively due to the length-scales involved, and information on technique optimisation has been limited. To address this, we have used AFM to characterise these networks and have developed a layer-by-layer fabrication protocol with precisely controlled layer thicknesses. Work to tailor the thin-film morphology by tuning the deposition parameters has also been performed. We show that spatial variations in the network morphology can be assessed using optical transmission scanning measurements. Finally, we have applied the focused ion beam – scanning electron microscopy nanotomography (FIB-SEM-NT) technique to reconstruct both 2D networks and heterostacks in 3D with unprecedented resolution. This allowed the internal structure of nanosheet films deposited under different conditions and using different nanosheet types to be characterised.

Contents

List of Figures

List of Tables

Es konnten keine Einträge für ein Abbildungsverzeichnis gefunden werden.

Abbreviations & Definitions

Abbreviation	Explanation
AFM	Atomic force microscopy
AR	Aspect ratio
EE	Electrochemical exfoliation
FIB-SEM-NT	Focused beam ion-scanning electron microscopy-nanotomography
LCC	Liquid cascade centrifugation
LS	Langmuir-Schaefer
SEM	Scanning electron microscopy
TEM	Transmission electron microscopy
TMDs	Transition metal dichalcogenides
TMMs	Transition metal monochalcogenides
TMTs	Transition metal trichalcogenides

1 Introduction

This deliverable mainly deals with characterisation results on the newly exfoliated layered material described in D1.5: “Production of novel 2D nanosheets” and solution-processed nanosheet networks and heterostacks described in D3.3: “Printed heterostructure fabrication”. The objective is to characterise the new materials to explore their fundamental properties and expand the 2D material library and to find reliable solutions to quantitively characterise the nanosheet networks and identify their features which can be used as a guidance for further network morphology optimization.

Theoretically predicted layered materials from D1.1 and D1.2 greatly expands our possible selections of materials. With crystals obtained from D1.3, exfoliation in liquids (liquid phase exfoliation and electrochemical exfoliation) has been performed in D1.5 to yield nanomaterials in suitable solvents. It is important to identify their morphology first as only materials with specific intrinsic mechanical properties could be exfoliated in such way. We performed a series of characterisations on these newly exfoliated nanomaterials, such as atomic force microscopy, transmission electron microscopy, to identify their two-dimensional nature (i.e., aspect ratio). Furthermore, the characterisation by Raman and UV-Vis optical spectroscopy will indicate their fundamental properties and allow us to gain more knowledge with them. In return, the experimental knowledge could be fed back into theoretical predication to narrow down the target parameters to find suitable layered materials.

Nanosheet inks can be solution-processed into networks, and here we mainly focus on Langmuir-Schaefer method, which employs the liquid-liquid interface to spontaneously form single-layered nanosheet networks (D3.3). The morphology of such networks has been rarely explored. Therefore, we adopted atomic force microscopy, (focused beam ion-) scanning electron microscopy (FIB-SEM), and optical transmission scanner to characterise their morphological information. The characterisation results are able to reveal properties such as thickness, pinhole density, film coverage, and film per perimeter length, etc. This allows us to be able to optimize the ink formulation and to find suitable conditions to achieve uniform, pinhole-free and ultra-thin nanosheet networks. With advanced characterisation techniques such as FIB-SEM, we could be able to quantitatively characterise the network information into its internal, e.g., porosity, which is not possible to be measured from its surface. Especially, when the interface is buried underneath, this method can still visualize the interface of interests.

Overall, a routine characterisation protocol with various techniques has been established. It is expected that more novel materials and networks from other tasks will be efficiently characterised. Other linked tasks will also commence, and it is believed that the objectives will be accomplished within the planned timeframe.

2 Methods

2.1 Background

The results presented in this deliverable report focus on the characterisation of initially available 2D materials, as well as their solution-processed networks and heterostacks. In this report, we characterise 2D materials that have been produced using liquid-phase exfoliation or electrochemical exfoliation in WP1, as well as their networks that were printed using an array of methods in WP3. The advanced characterisation techniques employed include scanning electron microscopy, atomic force microscopy, transmission electron microscopy, Raman and UV-Vis spectroscopy, and focused ion beam - scanning electron microscopy nanotomography. We will also show that the morphology of nanosheet thin films can be quantitatively assessed using optical transmission scanning measurements, which will inform future network and device optimisation. To assess the purity of the nanosheet surface, we established diffuse reflectance Fourier transform IR spectroscopy in the mid and far infrared as already outlined in D2.1.

2.2 Procedure

Nanosheet inks were produced using previously reported techniques of sonication-assisted liquid phase exfoliation[1] (LPE) and electrochemical exfoliation[2] (EE) using alkyl ammonium electrophiles as the intercalant. In both cases, the 2D inks were subjected to centrifugation to remove unexfoliated material, size-select the nanosheets, and facilitate solvent exchanges for printing. Characterisation using UV-vis spectroscopy, Raman spectroscopy, transmission electron microscopy (TEM), scanning electron microscopy (SEM) and atomic force microscopy (AFM) is part of routine workflows for the consortium and was applied according to standard protocols.

A high resolution optical flatbed scanner was used to measure the surface coverage and relative film perimeter length of printed thin-films. Images were captured at a resolution of 2400 dpi (pixel size ~ 10.6 µm). Pixel intensity values were converted to absolute transmittance, T, using a calibration curve determined using neutral density filters, and finally to optical extinction, Ext, using $Ext = -\log(T)$.

The nanostructure of printed 2D films and heterostacks was reconstructed in 3D using focused ion beam – scanning electron microscopy nanotomography (FIB-SEM-NT). The networks were imaged with voxel sizes of 5 × 5 × 15 nm, over representative volumes of $10^2 – 10^4$ µm^3.

2.3 Data Analysis

OriginPro was used for data analysis and visualization. Optical scanner images were processed and analysed using Python. FIB-SEM-NT cross-sections were segmented into their discrete components (e.g. pores and nanosheets) using Fiji, and the image stacks were aligned and compiled into 3D images using Dragonfly.

3 Results

3.1 Routine Nanosheet Characterisation

Following exfoliation, it is crucial to characterise the morphological and physicochemical properties of the nanosheets to ensure that the exfoliation has been completed and assess their suitability for device applications. To address this, we have characterised nanosheets produced using both electrochemical exfoliation and (sonication-assisted) liquid phase exfoliation using a variety of techniques. Transmission electron microscopy (TEM) was used to verify the morphology of LPE nanosheets such as $AsSbS_3$, As_2S_3, and SnGe (Fig. 1A-C). These were produced by ultra-sonication of the bulk powder in suitable liquids (e.g. N-Methyl-2-pyrrolidone) followed by size-selection through centrifugation. A similar picture was obtained when characterising nanosheets produced by wet-jet milling. The TEM images exemplarily shown in Fig. 1A-C display plate-like morphologies with lateral sizes on the order of hundreds of nanometres, verifying the 2D nature of the nanosheets and successful exfoliation.

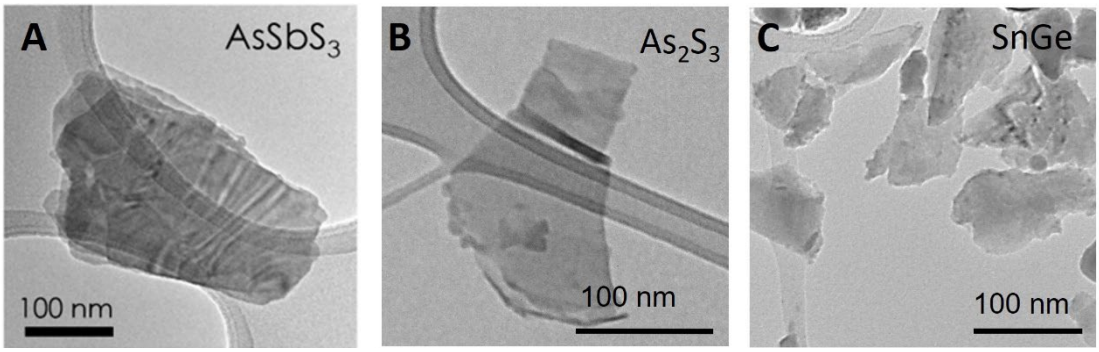

Figure 1: Transmission electron microscopy of liquid-exfoliated 2D materials. *TEM images of (A) $AsSbS_3$, (B) As_2S_3, and (C) SnGe nanosheets produced using liquid phase exfoliation.*

Electrochemical exfoliation was used to exfoliate bulk crystals from the transition metal mono- (TMM), di- (TMD) and tri-chalcogenide (TMT) families, including InSe, $Mo_{0.5}W_{0.5}Se_2$ and $HfSe_3$, respectively. Atomic force microscopy (AFM) was used to characterise the dimensions of the obtained nanosheets. A representative AFM image of EE InSe nanosheets on Si/SiO_2 is shown in Fig. 2A. In distinct contrast with the LPE nanosheets (Fig. 1), the EE InSe nanosheets in Fig. 2A exhibit lateral sizes of ~ 2-3 µm and thicknesses less than ~ 10 nm, meaning they are both larger and thinner. This was verified for the EE InSe, $MoWSe_2$ and $HfSe_3$ nanosheets by measuring the nanosheet length, L, and thickness, t, across many AFM images and plotting them against each other (Fig. 2B). Here, the data shows that the majority of the EE nanosheets have lengths > 1 µm and thicknesses < 10 nm. Such large and thin nanosheets lead to aspect ratios ($AR = L/t$) of $10^2 – 10^3$, as shown in Fig. 2C. The typical AR obtained by LPE is < 30 because the exfoliation mechanism is intrinsically limited by nanosheet mechanics[3]. Thus, the data shown in Fig. 2 is highly desirable from a printed electronics standpoint, where the mechanical flexibility and conformability of thin, high aspect ratio nanosheets is crucial to device performance.

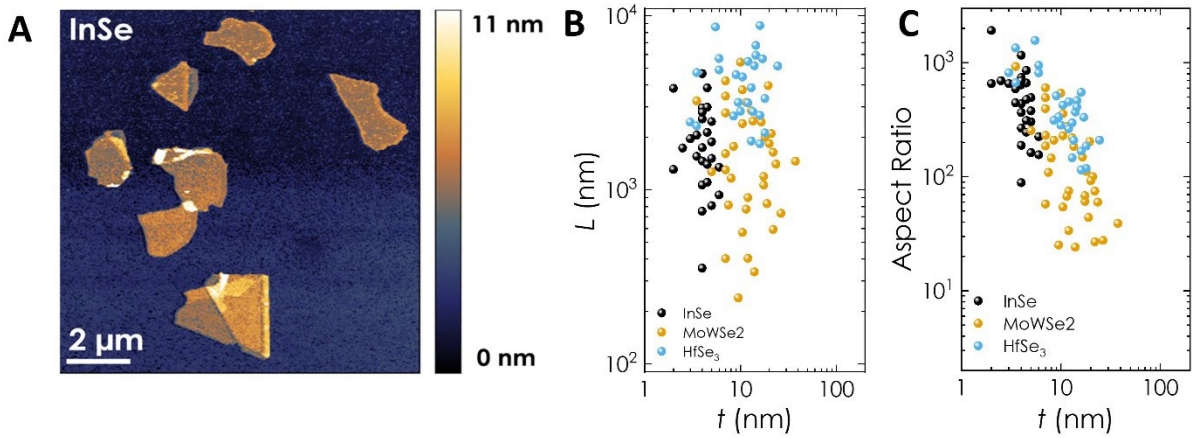

Figure 2: Atomic force microscopy of electrochemically exfoliated 2D materials*. (A) AFM image of EE InSe nanosheets on a Si/SiO_2 substrate. (B) The AFM-measured nanosheet length, L, plotted as a function of thickness, t, for EE InSe, $Mo_{0.5}W_{0.5}Se_2$, and $HfSe_3$ nanosheets. (C) The AFM-measured nanosheet aspect ratio (AR = L/t) for nanosheets from each material.*

The optical properties of the obtained EE nanosheets were investigated by UV-Vis optical spectroscopy and Raman spectroscopy. The absorption spectra of the nanosheet inks were collected using an integrating sphere and are shown in Fig. 3A. $HfSe_3$ shows absorption peaks at 444 nm and 514 nm. To our knowledge, the optical properties of $HfSe_3$ nanosheets have not previously been examined in detail. However, it is possible that the peaks are related to the excitation of charge carriers in the Se *p*-orbital valence states to the conduction band[4]. The $Mo_{0.5}W_{0.5}Se_2$ spectrum shows excitonic peaks that are similar to $MoSe_2$ and correspond to the A and B excitons at 798 nm and 658 nm, respectively[5]. InSe shows a broad peak at ~ 260 nm, which is consistent with the expected peak position from DFT calculations[6]. The Raman spectrum of $HfSe_3$ shows a A_g peaks at 202 cm^{-1}, 232 cm^{-1} and 253 cm^{-1}, which are likely attributed to the Ag vibrational mode[7]. The A_{1g} vibrational mode at ~ 247 cm^{-1} in $Mo_{0.5}W_{0.5}Se_2$ can be attributed to the out-of-plane motion of the Se atoms relative to a Mo or W atom, and a weak E_{2g} vibration at ~ 146 cm^{-1} is attributed to the in-plane vibrational motion of the Se atoms[8]. Finally, the A_{1g} (~ 117 cm^{-1} and 228 cm^{-1}) and E_{2g} (~180 cm^{-1}) vibrational modes for InSe are indicative of few-layer nanosheets. The A_{1g} mode is associated with the out-of-plane vibrations of the Se atoms, while the E_{2g} mode is due to in-plane vibrations between the In and Se in the basal plane.[9]

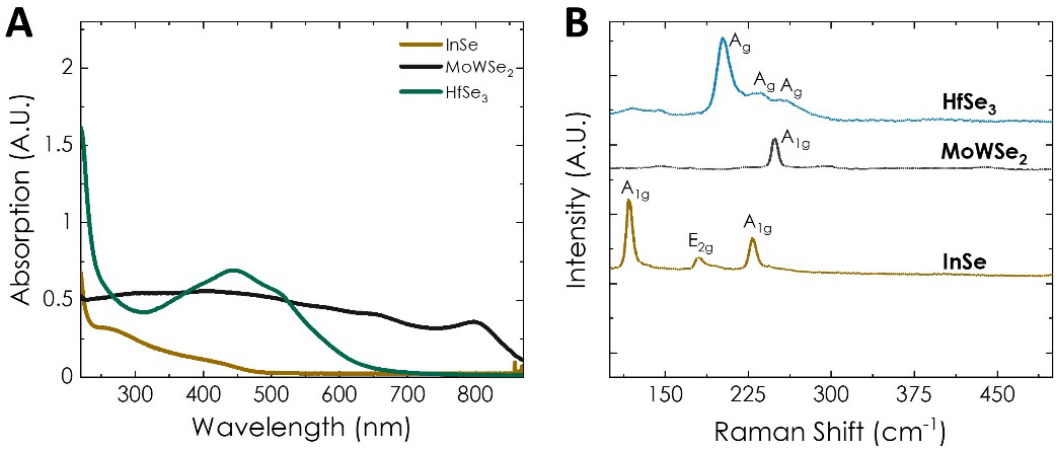

Figure 3: Spectroscopic characterisation of electrochemically exfoliated nanosheets. *(A) Absorption and (B) Raman spectra of InSe, $Mo_{0.5}W_{0.5}Se_2$, and $HfSe_3$.*

3.2 Spectroscopic Metrics

For LPE nanosheets, in particular TMDs, extinction and absorbance spectroscopy provides valuable information on the average nanosheet lateral size and thickness as we extensively investigated previously.[10-12] By linking the spectroscopic profile to the results from AFM statistical analysis, this allowed us to construct quantitative metrics to determine both average lateral size <L> and thickness <N> from extinction spectra. In the course of the project, we automated this analysis and now provide a freely accessible software solution for the automated analysis (https://github.com/S-Goldie/A2DfromUV).[13]

For EE nanosheets, no such metrics currently exist. Quantitative metrics derived for LPE nanosheets cannot be directly applied: On the one hand, nanosheets are laterally much larger so that edge effects cannot be used to assess <L>. On the other hand, the <N> metrics for LPE nanosheets rely on thickness dependent shifts of the excitons. However, EE nanosheets are often doped which leads to broadening and shifting of the excitons, or observation of trions rather than excitons. To gain a deeper understanding, we have produced ~20 dispersions of MoS_2 with different lateral size, thickness and doping level through changing the production conditions, in particular the intercalant. As exemplarily shown in Figure 4A, this can significantly change the extinction spectroscopic profile. In combination with extensive washing (see deliverable 2.1), we can also further vary the amount of doping from surface adsorbates which leads to a recovery of the A and B excitonic transitions (Figure 4B). We are currently elaborating in which way the exciton width, which can be extracted from fitting the second derivative (Figure 4C) can be linked to doping. Further, through a correlation with AFM statistics, we suggest a preliminary quantitative metric for thickness which is addressed through Milestone 12.

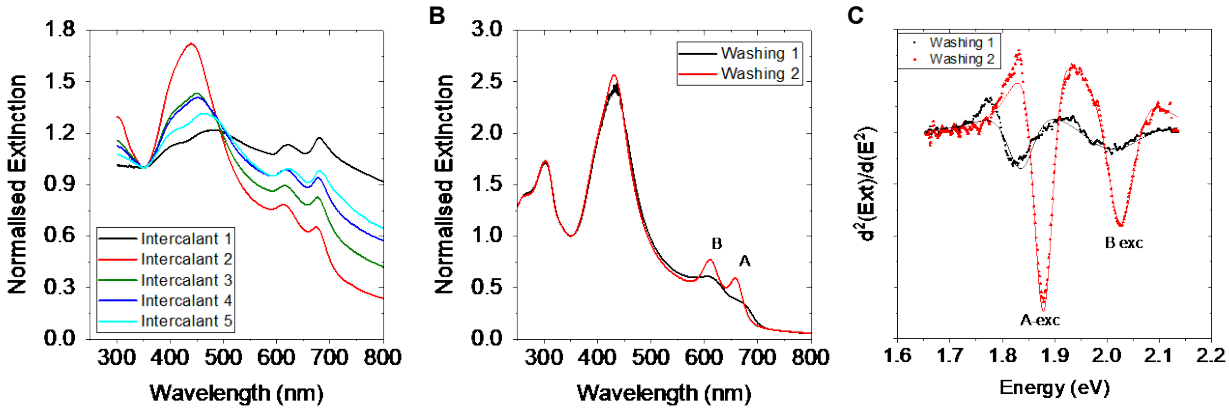

Figure 4: Extinction spectra of electrochemically exfoliated MoS_2 nanosheets. *(A) Extinction spectra of EE MoS2 produced with different intercalants. (B) Extinction spectra of the same EE MoS2 sample with different washing protocols to remove surface adsorbates. (C) Second derivative of the spectra in (B) fitted to the second derivative of two Lorentzian peaks to extract width and energy of the excitonic transitions.*

3.3 Characterisation of 2D Networks

To ensure that the physicochemical properties of nanosheets translate to their networks, it is critical that the network morphology can be characterised and optimised for a given application.
High aspect ratios are required for nanosheets to retain their mechanical flexibility, which facilitates the formation of aligned films with conformal junctions[14]. Scanning electron microscopy (SEM) was used to characterise the surface morphology of LS-deposited 2D networks comprised of nanosheets from Section 3.1 (Fig. 5). High-AR 2D materials such as EE InSe, $Mo_{0.5}W_{0.5}Se_2$ and $HfSe_3$ all display networks of well-aligned nanosheets with conformal large-area junctions, as shown in Fig. 5A-C, which are requirements for low junction resistances.

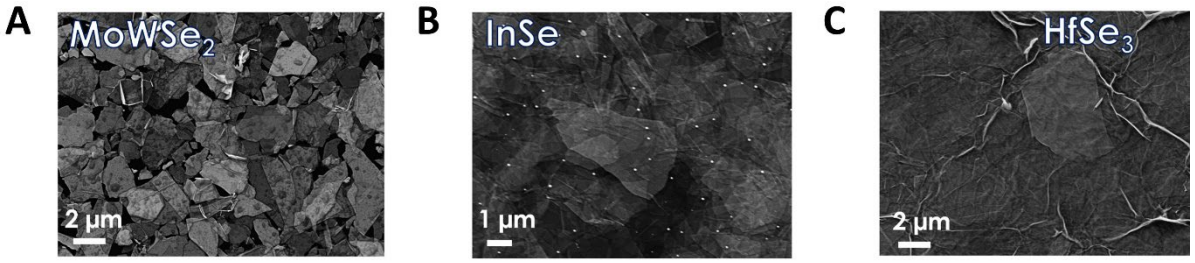

Figure 5: Scanning electron microscopy of LS-deposited EE nanosheet networks. *SEM images of thin films of (A) $Mo_{0.5}W_{0.5}Se_2$, (B) InSe, and (C) $HfSe_3$ nanosheets produced using electrochemical exfoliation and deposited using the LS technique.*

The LS technique that was used to deposit thin-films of EE nanosheets is shown schematically in Fig. 6A. This process relies on the spatial confinement of nanosheets at the interface of hexane and water to produce an atomically thin layer of nanosheets, which can then be deposited on a substrate passing through the interface. Here, EE MoS_2 nanosheets were used as the reference material for testing and optimising the LS technique. The obtained thin films were characterised by AFM, with an example image of a single layer of MoS_2 deposited on a glass substrate shown in Fig. 6B. To investigate potential redispersion effects and the viability of depositing thicker networks using the LS technique, sequential depositions of multiple EE MoS_2 layers were characterised using AFM.

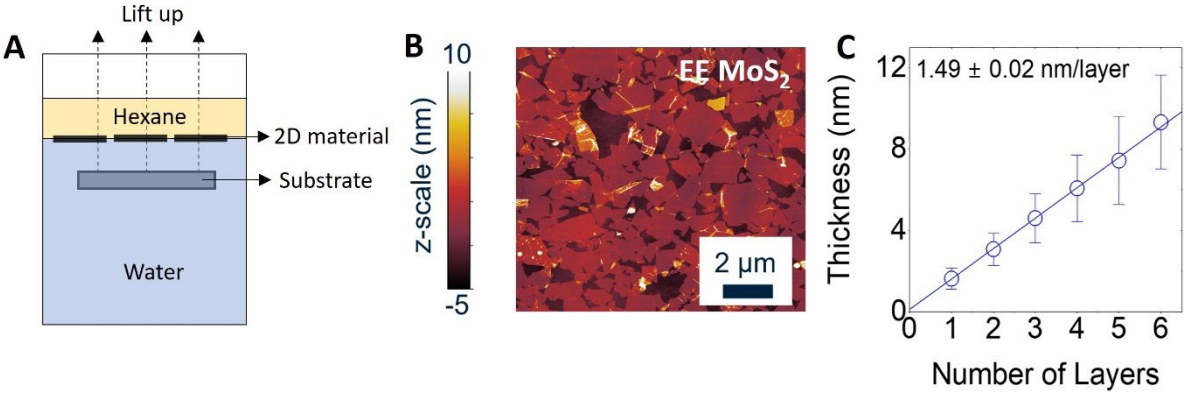

Figure 6: Characterisation of Langmuir-Schaefer deposited thin films*. (A) Schematic of the LS deposition process. (B) AFM image of a LS deposited single-layer EE MoS_2 film. (C) Film thickness versus number of deposition layers obtained from AFM.*

The film thickness was measured by AFM and plotted versus number of layers as shown in Fig. 6C. The film thickness increases linearly with the number of depositions, with an average layer thickness of

1.49 nm per LS deposition. This highlights that the thickness of LS-deposited EE MoS_2 networks can be precisely controlled and tailored for desired device applications.

Having shown this, it was then important to assess the surface coverage of LS-deposited nanosheet layers and ensure that closed and electrically percolating networks are formed. To address this, the surface coverage of a LS-deposited EE MoS_2 network was determined using SEM measurements (Fig. 7). By tuning the imaging conditions, the contrast between the nanosheets (grey) and substrate (white) can be greatly enhanced. This allows the SEM images to be segmented into its substrate and pore components, and the surface coverage to be measured quantitatively. Surface SEM characterisation on the single-layer LS MoS_2 thin film (Fig. 7) determined the surface coverage to be 79%. While this is reasonably high for a single LS deposition, it implies that there is significant scope for further optimization to achieve the conformal and pinhole-free network morphology that is required for next-generation printed 2D devices.

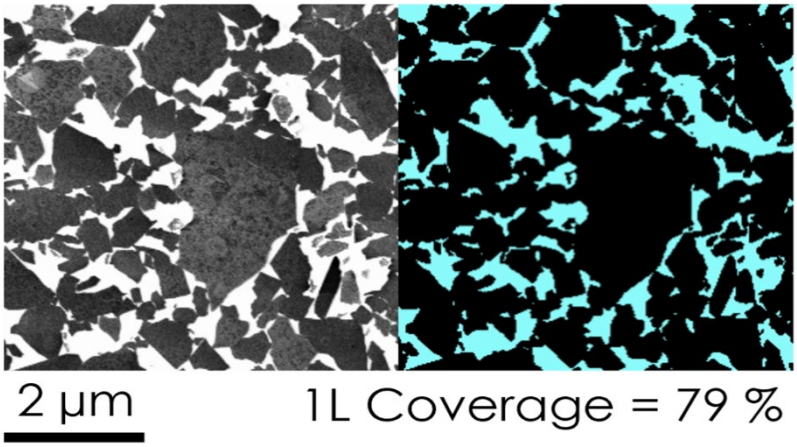

Figure 7: Characterisation of LS deposited EE MoS_2 films using scanning electron microscopy. *SEM image of a single-layer LS EE MoS_2 thin film (left) and its segmented image used to determine the relative surface coverage (right).*

To find the optimum fabrication conditions, graphene was used as a model material, which was also electrochemically exfoliated and LS-deposited onto glass substrates. The concentration of the graphene ink and the mass of graphene per unit area at the liquid-liquid interface were varied. For network characterisation, a commercial high-grade optical transmission scanner was used to evaluate the morphological information of the graphene films. A scanner was used in place of standard surface-analysis techniques, such as AFM or SEM, due to its significantly higher sample throughput and capability to perform quantitative analysis from the optical transmission signal. A series of optically-scanned EE graphene thin films with both varying ink concentration and areal mass loading are shown in Fig. 8A. For each scanned optical image, the transmission, *T*, histogram in the selected region was converted into extinction, *Ext*, by $Ext = -log(T)$, which is directly related to the thin film thickness, *t*, by $Ext = \varepsilon t$, where ε is extinction coefficient. Therefore, the thickness variation across the entire network could be detected from each optical transmission scan. As a result, we can evaluate morphological properties such as film coverage (Fig. 8B), which is determined by the integral of the peaks corresponding to exposed substrate ($\Sigma_{substrate}$), and the film (Σ_{film}), respectively. The coverage metric was taken from the ratio of both values ($1-[\Sigma_{substrate} / \Sigma_{film}]$) which quantifies the relative amount of the substrate covered by graphene, that a value of 1 indicates a complete coverage. Further, the film-

substrate perimeter length was obtained for a series of LS-deposited graphene films as a function of ink concentration and areal mass loading of nanosheets.

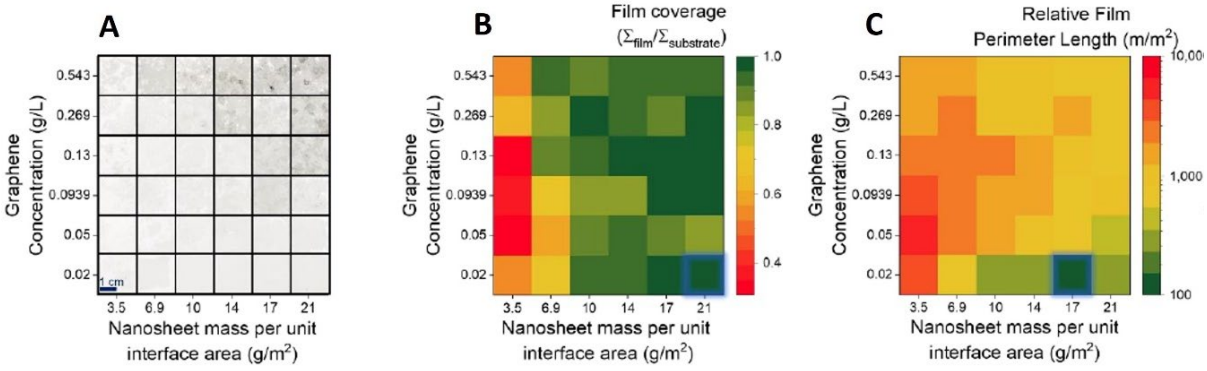

Figure 8: Optical characterisation of LS-deposited EE graphene thin films. *(A) Optically scanned image of graphene thin films on glass with varying concentration and mass per unit area. (B-C) Heat maps of (B) film coverage and (C) relative film perimeter length as a function of both graphene ink concentration and areal mass loading at the liquid-liquid interface.*

To this end, perimeter lengths were divided by the total area of the film to give a relative film perimeter length, which is shown in Fig. 8C. This quantifies the granularity of the film – a small relative perimeter length indicates a continuous film without pinholes. The heatmaps shown in Fig. 8B-C show a full coverage tends to be achieved at injection masses of ~17-21 g m^{-2} at all ink concentrations, while the relative nanosheet perimeter length is minimised for injections of 17 g m^{-2} at the lowest concentration studied to this point (0.02 g L^{-1}). Work to further expand the parameter space for optimisation is underway.

3.4 3D Imaging of 2D Networks and Heterostacks

To fully realise the potential of printed 2D networks and heterostacks for device applications, the ability to quantitatively characterise their internal nanostructure and interfacial properties will be critical. We are working to develop the focused ion beam – scanning electron microscopy nanotomography (FIB-SEM-NT) technique to reconstruct printed nanosheet networks in 3D with voxel sizes of 5 × 5 × 15 nm^1. This allows the internal morphological properties of these systems to be analysed in a way that is inaccessible to other surface characterisation techniques (AFM, SEM), or lower resolution tomography techniques (X-ray CT). Here, FIB-SEM-NT has been used to quantitatively assess the morphology of printed 2D networks and heterostacks of initially available 2D materials deposited using different techniques.

3D reconstructions of spray-coated LPE and EE graphene nanosheet networks deposited under similar conditions are shown in Figs. 9A-B, respectively. The resolution afforded by FIB-SEM-NT allows the morphological differences between these networks to be resolved. Individual nanosheets and pores can be resolved in the spray-coated LPE graphene network (Fig. 9A), while the larger aspect EE graphene nanosheets conformally overlap to form a densely packed monolithic network, shown in Fig. 9B. This results in a ~ 20-fold reduction in the network porosity in the spray-coated network of EE nanosheets (P_{Net} ~ 2 %), when compared to its LPE counterpart (P_{Net} = 43 %). Such conformal stacking and this reduction in porosity leads to a ~ 5-fold decrease in the surface roughness going from the spray-coated LPE graphene network (R_{RMS} = 214 nm) to the EE graphene film (R_{RMS} = 42 nm). This has implications for improved layer and interfacial properties in printed heterostacks and devices, which can be characterised using FIB-SEM-NT.

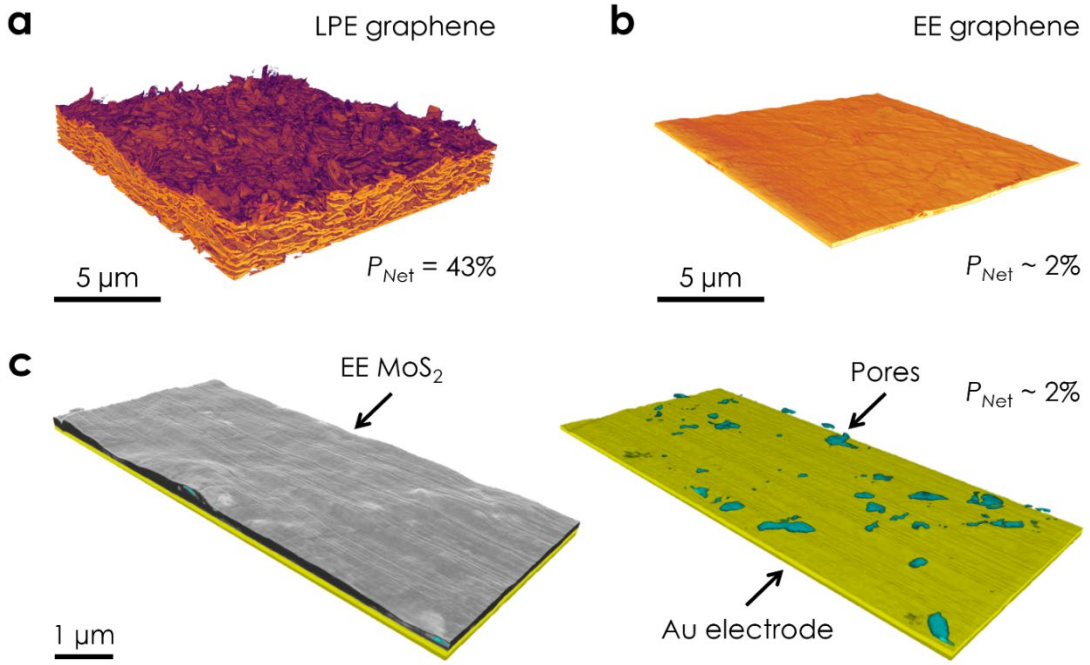

Figure 9: 3D reconstructions of printed 2D networks generated using FIB-SEM nanotomography. *(A-B) 3D reconstructions of (A) LPE and (B) EE graphene nanosheet networks that were spray coated under similar conditions. (C) 3D reconstruction of LS-deposited EE MoS_2 nanosheets on an evaporated gold electrode. Both the nanosheet and pore contributions to the LS-deposited 2D network are shown. The network porosity, P_{Net}, is given for each network in (A-C).*

A a network of LS-deposited EE MoS_2 nanosheets on a gold electrode is shown in Fig. 9C. Here, the nanosheet and pore contributions have been isolated to reveal the internal nanostructure of the LS-deposited film on the gold electrode. As with the sprayed EE graphene network shown in Fig. 9B, a conformally tiled network of high-aspect ratio of EE MoS_2 nanosheets is shown for the LS-deposited film in Fig. 9C. This results in a network mesoporosity of P_{Net} ~ 2 %, with only a few isolated pores present inside the 2D network. Work to develop protocols for additional characterisation methodologies for printed 2D networks using FIB-SEM-NT is currently in progress.

3.5 Contribution to project (linked) objectives

The current deliverable will contribute to the entire project. Especially we can use the information from the nanosheet characterisation to further explore more types of layered crystals with desired properties. To this end, standard characterisation techniques are in place (TEM, SEM, AFM, extinction/absorbance, Raman, IR spectroscopy, EDX) and will be complemented with more advanced techniques in ongoing work (XPS, TOF-SIMS, UPS, LEIPS). The development of high throughput spectroscopic metrics will be key to optimise the ink production process beyond concentration. In particular, this will allow us to gain insights into the mechanism of electrochemical exfoliation to be able to rationally control nanosheet lateral sizes, thicknesses, aspect ratios and doping.

The characterisation on networks will enable us to visualize the network morphology and identify and adjust the optimum conditions to realize the ideal thin film morphology. This will be crucial to optimise device performance. The characterisation protocols developed in this deliverable will also be applicable to the other tasks in the project, e.g. tasks related to functionalisation.

3.6 Contribution to major project exploitable result

Not applicable

4 Conclusion and recommendation

In conclusion, we present our characterisation results on novel exfoliated nanosheets and their networks and heterostacks formed by the LS method. The exploited nanosheets include LPE $AsSbS_3$, As_2S_3, and SnGe, and EE InSe, $Mo_{0.5}W_{0.5}Se_2$, and $HfSe_3$. It is found that the obtained nanosheets from EE give much higher aspect ratio than those made from LPE. These large aspect ratio nanosheets would be beneficial when forming networks due to their flexibility. Their basic properties were also investigated by XRD, UV-Vis, and Raman spectroscopy. As more novel layered materials are expected to be soon exfoliated, the library of the new 2D materials will be expanded. Further, we are working on quantitative metrics for EE MoS_2 to assess thickness and doping. Once established, we aim to establish a metrics library for different materials in analogy to our previous work on LPE nanosheets.

The LS method is believed to be a reliable method to allow nanosheets to tile on each other and form atomically thin but continuous thin films. We adopted AFM and SEM to characterise thin films made from EE nanosheets. It is found that the film thickness can be tuned by only single layer thick with each deposition layer. The thin film morphology was further characterised by an optical transmission scanner to find spatially variation of film thickness. This allows us to probe information of film coverage and relative film perimeter length. The obtained result can help with optimization of thin film deposition. Using advanced characterisation technique, such as FIB-SEM-NT, the internal nanosheet network can be revealed and the porosity of the network can be quantitatively calculated from the image. Further, the buried interface of the heterostacks can be visualized.

5 Risks and interconnections

5.1 Risks/problems encountered

Not applicable

5.2 Interconnections with other deliverables

The current deliverable is closely related to the upcoming deliverables D4.2 “Characterization of new materials identified through theory” and D4.3 “Protocols for new characterization methodologies”.
Some aspects of the characterisation using diffuse reflectance Fourier transform infrared spectroscopy in the mid- and far-infrared to assess surface adsorbates and functionalisation were reported on in D2.1.
Since characterisation of nanosheets and their networks is an integral part of the process chain from production to applications, it is directly or indirectly connected to all tasks and deliverables within 2D-Printable.

6 Deviations from Annex 1

Not applicable

7 References

1 Kaur, H. *et al.* Liquid-Phase Exfoliation of Arsenic Trisulfide (As2S3) Nanosheets and Their Use as Anodes in Potassium-Ion Batteries. *ACS Nano*, doi:10.1021/acsnano.4c03501 (2024).

2 Carey, T. *et al.* High-Mobility Flexible Transistors with Low-Temperature Solution-Processed Tungsten Dichalcogenides. *ACS Nano* **17**, 2912-2922, doi:10.1021/acsnano.2c11319 (2023).

3 Backes, C. *et al.* Equipartition of Energy Defines the Size-Thickness Relationship in Liquid-Exfoliated Nanosheets. *ACS Nano* **13**, 7050-7061, doi:10.1021/acsnano.9b02234 (2019).

4 Pacilé, D. *et al.* Photoemission and optical studies of ZrSe3, HfSe3 and ZrS3. *Phys. Rev. B* **76**, 155406, doi:10.1103/PhysRevB.76.155406 (2007).

5 Dong, N. *et al.* Optical Limiting and Theoretical Modelling of Layered Transition Metal Dichalcogenide Nanosheets. *Sci. Rep.* **5**, 14646, doi:10.1038/srep14646 (2015).

6 Shang, J. *et al.* Tunable electronic and optical properties of InSe/InTe van der Waals heterostructures toward optoelectronic applications. *J. Mater. Chem. C* **6**, 7201-7206, doi:10.1039/C8TC01533C (2018).

7 Zwick, A., Renucci, M. A. & Kjekshus, A. Raman scattering in the IVB transition-metal trichalcogenides: ZrS3, ZrSe3, ZrTe3 and HfSe3. *J. Phys. C: Solid State Phys.* **13**, 5603, doi:10.1088/0022-3719/13/30/023 (1980).

8 Dey, S. & Singh, G. Sodium and potassium ion storage in cation substituted 2D MoWSe2: insights into the effects of upper voltage cut-off. *Nanotechn.* **34**, 385401, doi:10.1088/1361-6528/acdf66 (2023).

9 Lei, S. *et al.* Evolution of the Electronic Band Structure and Efficient Photo-Detection in Atomic Layers of InSe. *ACS Nano* **8**, 1263-1272, doi:10.1021/nn405036u (2014).

10 Backes, C. *et al.* Edge and Confinement Effects Allow in situ Measurement of Size and Thickness of Liquid-Exfoliated Nanosheets. *Nature Commun.* **5**, 4576 (2014).

11 Backes, C. *et al.* Production of Highly Monolayer Enriched Dispersions of Liquid-Exfoliated Nanosheets by Liquid Cascade Centrifugation. *ACS Nano* **10** 1589-1601 (2016).

12 Synnatschke, K. *et al.* Length and thickness dependent optical response of liquid-exfoliated transition metal dichalcogenides. *Chem. Mater.* **31**, 10049-10062 (2019).

13 Kubetschek, N., Backes, C. & Goldie, S. Algorithm for Reproducible Analysis of Semiconducting 2D Nanomaterials Based on UV-VIS Spectroscopy. *Adv. Mater. Interfaces* **n/a**, 2400311, doi:https://doi.org/10.1002/admi.202400311.

14 Kelly, A. G., O'Suilleabhain, D., Gabbett, C. & Coleman, J. N. The electrical conductivity of solution-processed nanosheet networks. *Nature Rev. Mater.* **7**, 217-234, doi:10.1038/s41578-021-00386-w (2022).

8 Acknowledgement

The author(s) would like to thank the partners in the project for their valuable comments on previous drafts and for performing the review.

Project partners:

#	Partner short name	Partner Full Name
1	TCD	TCD THE PROVOST, FELLOWS, FOUNDATION SCHOLARS & THE OTHER MEMBERS OF BOARD, OF THE COLLEGE OF THE HOLY & UNDIVIDED TRINITY OF QUEEN ELIZABETH NEAR DUBLIN
2	UNISTRA	UNIVERSITE DE STRASBOURG
3	UKa	UNIVERSITAET KASSEL
4	BED	BEDIMENSIONAL SPA
5	TUD	TECHNISCHE UNIVERSITAET DRESDEN
6	VSCHT	VYSOKA SKOLA CHEMICKO-TECHNOLOGICKA V PRAZE
7	UNR	UNIRESEARCH BV
8	UniBw M	UNIVERSITAET DER BUNDESWEHR MUENCHEN
9	EPFL	ECOLE POLYTECHNIQUE FEDERALE DE LAUSANNE

Disclaimer/ Acknowledgment

This project has received funding from the European Union's Horizon Europe research and innovation programme under grant agreement No 101135196. Views and opinions expressed are however those of the author(s) only and do not necessarily reflect those of the European Union. Neither the European Union nor the granting authority can be held responsible for them.

9 Appendix A - Quality Assurance Review Form

The following questions should be answered by all reviewers (WP Leader, reviewer, Project Coordinator) as part of the Quality Assurance procedure. Questions answered with NO should be motivated. The deliverable author will update the draft based on the comments. When all reviewers have answered all questions with YES, only then can the Deliverable be submitted to the EC.

NOTE: This Quality Assurance form will be removed from Deliverables with dissemination level "Public" before publication.

Question	**WP Leader**	**Reviewer**	**Project Coordinator**
	Claudia Backes (UKa)	Georg Duesberg (UNIBW M)	Jonathan Coleman (TCD))
1. *Do you accept this Deliverable as it is?*	Yes	Yes	Yes
2. *Is the Deliverable complete?* - *All required chapters?* - *Use of relevant templates?*	Yes	Yes	Yes
3. *Does the Deliverable correspond to the DoA?* - *All relevant actions preformed and reported?*	Yes	Yes	Yes
4. *Is the Deliverable in line with the 2D-PRINTABLE objectives?* - *WP objectives* - *Task Objectives*	Yes	Yes	Yes
5. *Is the technical quality sufficient?* - *Inputs and assumptions correct/clear?* - *Data, calculations, and motivations correct/clear?* - *Outputs and conclusions correct/clear?*	Yes	Yes	Yes
6. *Is created and potential IP identified and are protection measures in place?*	NA	NA	NA
7. *Is the Risk Procedure followed and reported?*	NA	NA	NA
8. *Is the reporting quality sufficient?* - *Clear language* - *Clear argumentation* - *Consistency* - *Structure*	Yes	Yes	Yes